Four-body L=1 systems from contact EFT

Lorenzo Contessi,[1, *] Jaume Carbonel,[2] Johannes Kirscher,[3] Rimantas Lazauskas,[4] and Martin Schäfer[5]

[1] *IRFU, CEA, Université Paris-Saclay, 91191 Gif-sur-Yvette, France*
[2] *Université Paris-Saclay, CNRS/IN2P3, IJCLab, 91405 Orsay, France*
[3] *Theoretical Physics Division, School of Physics and Astronomy,*
The University of Manchester, Manchester, M13 9PL, UK
[4] *IPHC, IN2P3-CNRS/Université de Strasbourg BP 28, F-67037 Strasbourg Cedex 2, France*
[5] *Nuclear Physics Institute of the Czech Academy of Sciences, 25069 Řež, Czech Republic*
(Dated: March 28, 2022)

Scattering resonances are ubiquitous in physics, and for the understanding of the behaviour of few-body quantum systems as important as bound states. Compared with the latter, their theoretical handling and their role in the interpretation of data is complicated through their unstable nature which is reflected in their belonging to the continuum spectrum. The smallest nuclear system comprised solely of resonances is 4-hydrogen with $L = 1$ states about 3.5 MeV above the triton-neutron threshold.

In this article, we analyze the minimal contact theory which predicts such P-wave, four-body resonances. Furthermore, we establish numerically the emergence of this specific resonance pole for a wider class of systems whose two-body scale is significantly larger ($\to \infty$) than their interaction range. Specifically, we employ a contact effective field theory renormalized with nuclear observables (LO pionless effective field theory) and to unitary systems without a finite two-body scale (universal contact effective field theory). We find a negative-parity four-body resonance pole which is stable with respect to the short-distance structure of the regularized two- and three-body momentum-independent contact potentials with three independent numerical algorithms: a finite-volume Gaussian-stochastic-variational technique, the solution of the AGS on a discrete coordinate-space grid, and a one-channel, two-body, resonating-group reduction of the problem. Thereby we demonstrate that a zero-range potential provides a non-trivial pole structure for the four-body amplitude.

I. INTRODUCTION

Resonance phenomena occur ubiquitously in quantum and classical physics. Relative to stable bound states, their handling in many-particle hadronic, nuclear, and atomic physics is complicated. A resonance results from a nonperturbative interplay of particle-particle interactions, fine-tuned potential shapes, and channel couplings that lead to multiple excitations and thresholds. Relative long life times and energies very close to production thresholds lead to clean, measurable signals, while in practise, a rapid decay and an energy far from threshold makes their identification with cross section data involved. Theoretically, the structure of a Hamiltonian usually does not expose the existence of resonances without explicitly solving dynamical equations. In the latter course, numerical methods to extract complex energies are, in general, expensive and less accurate compared with those for bound states.

In order to identify general features of an interaction which allow for the prediction of resonances, we focus on the 4-hydrogen (^{4}H), the smallest nuclear system known to be characterized by a resonance. In this system, $J^\pi = 0^-, 1^-, 2^-$ resonances are found experimentally approximately 5.2 MeV, 3.5 MeV, and 3.2 MeV, respectively, above the triton-neutron threshold. Cross sections and scattering parameters have been studied extensively both experimentally [? ? ?] and theoretically [? ? ? ? ? ?]. The position of the ^{4}H, $J^\pi = 1^-$ resonance pole was located in Refs. [? ? ?] at an energy $Re(E) = \{0.90 - 1.23\}$ MeV and width $\Gamma = \{3.5 - 5.8\}$ MeV. From data, a R-matrix analysis puts this pole at $Re(E) = 3.50$ MeV and $\Gamma = 6.73$ MeV [?]. Despite the quantitative discrepancy among theory and experiment, the sheer existence of the pole in different models is remarkable. Why does such a pole emerge in the four-body amplitude but is absent, e.g., in the deuteron-neutron quartet channel or the three-neutron system? What are minimal conditions and characteristics of the employed models necessary for these features? These questions are crucial in the development of the nuclear effective field theory in order to make it useful for the description of heavier nuclei beyond the S shell. Furthermore, fermi statistics which enforces higher relative angular momenta in ground-state wave functions of more than four nucleons, is equally relevant for hadronic, atomic, in general, all fermions amenable to a description with zero-range forces. Hence, an understanding how the structure of these forces leads to

---

* lorenzo@contessi.net

Nuclear LECs			Universal LECs		
Λ [fm^{-1}]	C_0 [MeV]	D_0 [MeV]	Λ	C_0	D_0
1	-44.4552	27.2312	1	-0.671	0.678
2	-142.376	172.703	2	-2.684	7.749
3	-295.959	559.013	4	-10.736	194.253
4	-505.202	1397.56	6	-24.156	4273.294
6	-1090.66	6311.30	8	-42.944	122391.358
10	-2929.48	89436.2	10	-67.100	4102409.239

TABLE I: LECs fitted for each cut-off. In the left tab are listed the LECs fitted to reproduce deuterium and ^{3}He energy in MeV. On the right the ones that reproduce unitary systems of nuclei.

certain few-body resonance poles carries value far beyond the ^{4}H system, namely: is a leading-order description of a system of particles, whose statistics demand mixed-orbital-symmetry states, with properly renormalized coupling strengths of zero-range, possibly spin-/flavour-dependent interactions possible?

Such renormalizable effective field theories (EFT) were instrumental in understanding the relation between nuclear physics and its underlying theory of quantum chromodynamics and for deriving universal features which nuclei share with atoms. All EFT's comprise of the most general Lagrangean whose terms are built with appropriately chosen degrees of freedom and meet certain internal and space-time symmetries. A hierarchy (power counting) amongst this infinity of operators and their weight within an iterative expansion of the S-matrix renders the theory *effective*, i.e., useful. In the two-body sector, the convergence of the expansion and the choice of the relevant degrees of freedom depends on the typical momentum exchanged between interaction partners; for different typical momenta, different EFT expansions are needed. For instance, few-body nuclear systems are close to the unitary limit, where the two-body scattering length is much larger than any other scale, an expansion around an infinite (or large) scattering length with solely nuclear degrees of freedom yields the bulk structure of nuclei up to 4-helium [?]. For momenta that allow for the creation of pions, this pion-less power counting (EFT($\not\pi$)) fails. For these momenta, chiral EFTs couple the pion field to the nucleons and thereby introduce long-range forces at leading order, while EFT($\not\pi$) is of zero-range at leading order and thus easier to treat numerically and analytically. Whether this simplicity of a zero-range theory still does not lead to an exclusion of complex many-body phenomena, e.g., shallow quantum states and resonance poles is unknown and shall be studied in this article.

What is known about EFT($\not\pi$) , in particular, is its ability to predict the behavior of many-boson systems and nuclei up to four nucleons. However, the leading order (LO) of the theory cannot account for the observed behavior of multi-fermionic systems. There, it erroneously predicts unbound nuclei above four particles, e.g. ^{7}Li and ^{16}O [? ?]. It was conjectured more generally, that zero-range theories cannot sustain bound states of mixed symmetry. However, the bound character of a state might appear only at a higher orders of the EFT provided that the LO creates a pole of other kind, virtual or resonant, which the modification of the interaction at higher order transforms into a bound state. If no such pole is present at LO in these systems – of which ^{4}H is the smallest – only a modification of the power counting will furnish the correct description of nuclear physics with contact EFTs.

The creation of resonant S-wave poles at LO EFT($\not\pi$) was demonstrated in case of the hyper triton ($nn\Lambda$) in Ref. [?] (as a subthreshold resonance) but there is no record of such poles being created renormalization-scheme independently in systems with mixed symmetry ground states such as ^{4}H with a zero-range theory. It is the aim of this work to analyze this creation of a four-body P-wave resonance pole from an zero-range, spherically-symmetric regularized contact interaction with coupling strengths resembling nuclear systems close to unitarity and also systems which realize this limit with an infinite two-body scattering length, i.e., zero-energy bound state.

In the following section, we introduce the Hamiltonian of the theory along with comments on its solution with a Gaussian-stochastic-variational method, the treatment of the scattering problem via the Alt, Grassberger, and Sandhas equations in coordinate space, and the reduction of N-body, two-fragment scattering onto a two-body problem. Following this, we present results for effective-range parameters and pole positions for the low-energy scattering of a neutron on ^{3}H before generalizing this to a generic point particle impinging on a universal trimer. Finally, we relate the regulator independence of the results to the deployed minimal theory as a first-order approximation of nuclei and universal, unitary systems.

II. CONTACT EFT AND NUMERICAL METHODS

The minimal theory for the

The leading order (LO) of the contact EFT we are employing consists of a contact two-body and a contact three-body operators with two low energy constants (LECs) to be fitted on physical observables [?]. A Gaussian regulator

and a cut-off Λ are introduced to smear the potential such that the contact limit is restored for $\Lambda \to +\infty$:

$$V(\mathbf{r}) = C_0 \sum_{i,j}^{N} e^{-\frac{r_{ij}^2 \Lambda^2}{4}} \tag{1}$$

$$W(\mathbf{r}) = D_0 \sum_{ijk}^{N} \left[e^{-\frac{(r_{ij}^2 + r_{ik}^2)\Lambda^2}{4}} + e^{-\frac{(r_{ij}^2 + r_{jk}^2)\Lambda^2}{4}} + e^{-\frac{(r_{jk}^2 + r_{ik}^2)\Lambda^2}{4}} \right]. \tag{2}$$

Once the interaction is regularized the LECs (C_0 and D_0) become cut-off dependent and must be fitted for any Λ to reproduce the chosen set of fixed two- and three-body observables. Nonetheless, if the theory is renormalizable this is sufficient to stabilize (in the sense of converging to a finite value) any other few- and many-body observable in the *large cut-off limit*. We employ two different two-body potentials in this study, a central one and one projected in S-wave only. This division is necessary for the numerical methods we use but is relevant only for small cut-offs. In fact, in the limit, $\Lambda \to \infty$, the projected and unprojected potentials converge to the same contact interaction essentially representing only a different choice of the regulator. Nonetheless, for small cut-off we expect and experience discrepancies, this results especially in different sets of three-body LEC D_0 that fix the three-body energy. Moreover, for each projected and unprojected interaction we fit two sets of LECs. The first, the "nuclear" one, fixes a single two-body boundstate of $B_2 = 2.22$ MeV (both in singlet and triplet channels). In the second, the "universal" ones, the LECs are fitted to reproduce a large two-body scattering length ($a_0 > 10^5$). In both cases, the three-body is fitted to reproduce a single three-body boundstate $B_3 = -8.482$ MeV, and we employ the same nucleon mass to $m = 938.858$ MeV, and the same $\hbar c = 197.31613$. As an example, in tab. I, we report the nuclear and universal LECs for the unprojected interaction.

Since EFT($\not{\pi}$) is best suited for the description of low energy observables we refer to the effective range expansion (ERE) scattering parameter. It is essentially the expansion in low momentum of the phaseshift of a relative angular momentum L two-body problem phaseshift δ:

$$k^{2L+1} cot(\delta) = -\frac{1}{a_L} + \frac{1}{2} r_L k^2 + \dots . \tag{3}$$

The same expansion can be used either in the two-body problem and in the four-body one assuming that ^{4}H can be seen as a $n-^3$H pair. Resonances will therefore emerge as poles of the system T-matrix

$$T = \frac{1}{k^{2L+1} cot(\delta) - ik} \tag{4}$$

and can be extracted either by fitting phaseshifts to the ERE formula or directly through solving the Schrödinger equation for complex energies.

Numerical methods

In this work, we utilize three different methods to solve the $n-^3$H shröedinger equation. The Rimas Method, the Stochastic Variational Method, and the Resonating Group Method. Coupled with these technologies we use also the complex rotation and the Analytic Continuation of the Coupling Constant (ACCC) to determine the position of resonant solution of the four-body problem (belonging to the continuum and hard to be extracted with the conventional methods) and the scattering lengths and volumes of the $n -^3 H$ reaction.

wrong and to be changed SVM consists of the variational search of the ground state of the problem using an over-complete set of Gaussians, chosen stochastically for each Jacobi coordinate, to represent the system wave function. This few-body method was developed by Lee Suzuki [] in ... and refined during the years to provide a reliable and relatively cheap solver for ground-state system up to ~ 6 particles. A review of the method can be found in [] and a deeper insight is given by [].

III.   PROCEDURE AND RESULTS

Our discussion begins with the analysis of low energy scattering parameters of the $n-^3$H system. This system allows for several low-energy states with relative angular momentum $J = 1$ between the fragments: 0^-, 1^-, and 2^-;

Scattering lengths and volumes
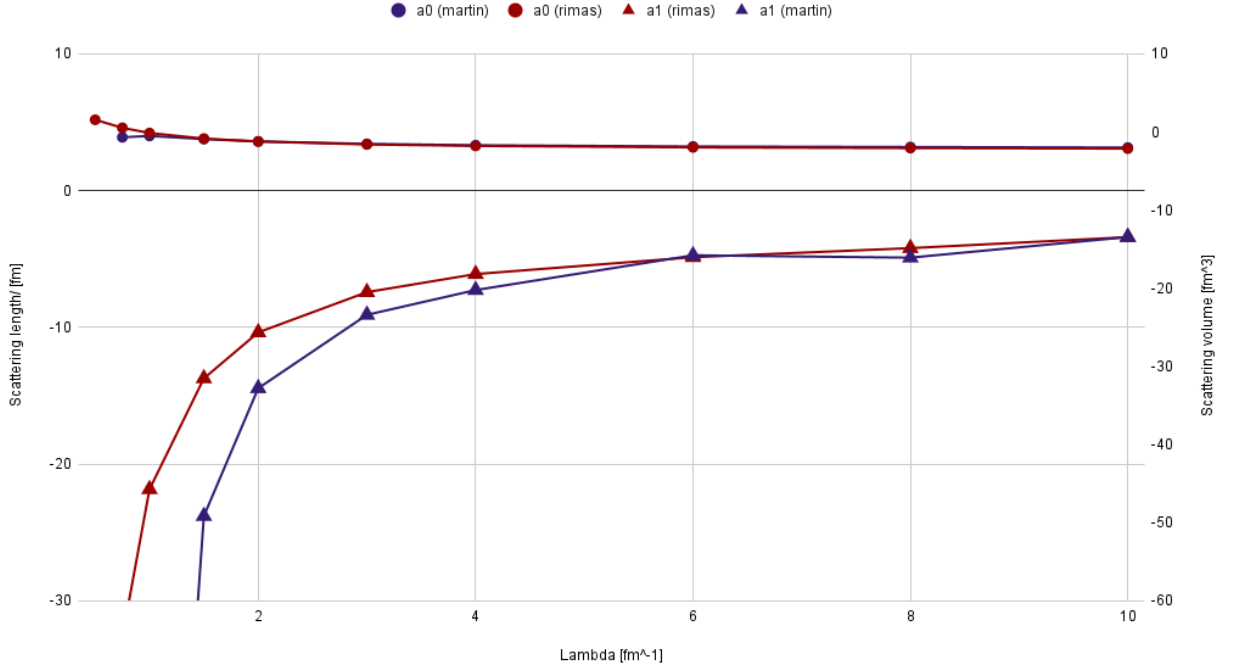
FIG. 1: 1^- resonant pole in ^{4}H

we focus exclusively on the natural parity state: 1^-. We also study the state 0^+, with relative angular momentum L=0. This state is Pauli excluded, therefore, we do not expect any resonant or bound state in this channel but we still consider it interesting to study the EFT behavior and as a benchmark among different methods. In figure 1 we shown the scattering length and volume (relative to 0^+ and 1^- states) calculated using SVM and RIMAS microscopical approaches. Can be noticed how, for large enough cutoffs, the two methods are compatible. This was expected since the two calculations use effectively two different regulators due to the presence of an S-wave projected and unprojected two-body potential. The difference between the two is more noticeable in the $J^\pi = 1^-$ channel as the effect of P-wave interactions is more evident. The two scattering parameters converge with the cut-off to a finite value. This fact is nontrivial since the interparticle interaction converges to a contact potential for large cut-offs. In fact, n and ^3H contain an identical fermion which suppresses any positive parity interaction. However, the contact nature of the potential allows only particles in relative S-wave to interact. The finiteness of a_0 and a_1 should, therefore, be explained by the mediation of the distinguishable fermions and by the few-body effects. a_0 and a_1 converge, empirically, as $1/\lambda$. In other words, since the interplay of S-wave interactions can result in a finite interaction in P-wave among few-body clusters, the scattering length/volume remains finite even only including the theory LO. As a consequence, their cut-off behavior is $\propto 1/\Lambda$ as expected by LO observables. The sign and magnitude of the converged results ($a_0 \simeq 3.1$ fm and $a_1 \simeq -13(1)$) indicate the absence of boundstates, but the a_1 magnitude might indicate the presence of a shallow pole in the 1^- system. It is also interesting to notice that the effective range for 0^+ and 1^- remains also finite ($r_0 \simeq 2$ fm and $r_1 \simeq 1$ fm respectively). This is also expected since, despite the nucleon-nucleon interaction is of contact nature, the size of the fragments remains finite, allowing for an inter-fragment long-range effect.

While arguably the best method to extract phaseshifts and resonance positions, the microscopic approach becomes more and more complicated and unfeasible when the number of particles is increased. For this, we would like to tackle the same problem from a different perspective: using the RGM formalism. RGM intrinsically contains an approximation in the form of a simplified few-body wave function of one of the fragments. It is, however, easily extendable to larger systems. In our case, RGM transform a four-body problem into a simplified two-fragment one at the price of

The second step in our calculation is the determination of the $J^\pi = 1^-$ nuclear resonance position in the Energy complex plane. This has been done using the ACCC method starting from "RIMAS" numerical method. In figure 3, the evolution of such pole can be follow to pass the threshold energy $B_t = 8.484$ MeV ($Re(E) = 0$ in the plot) to
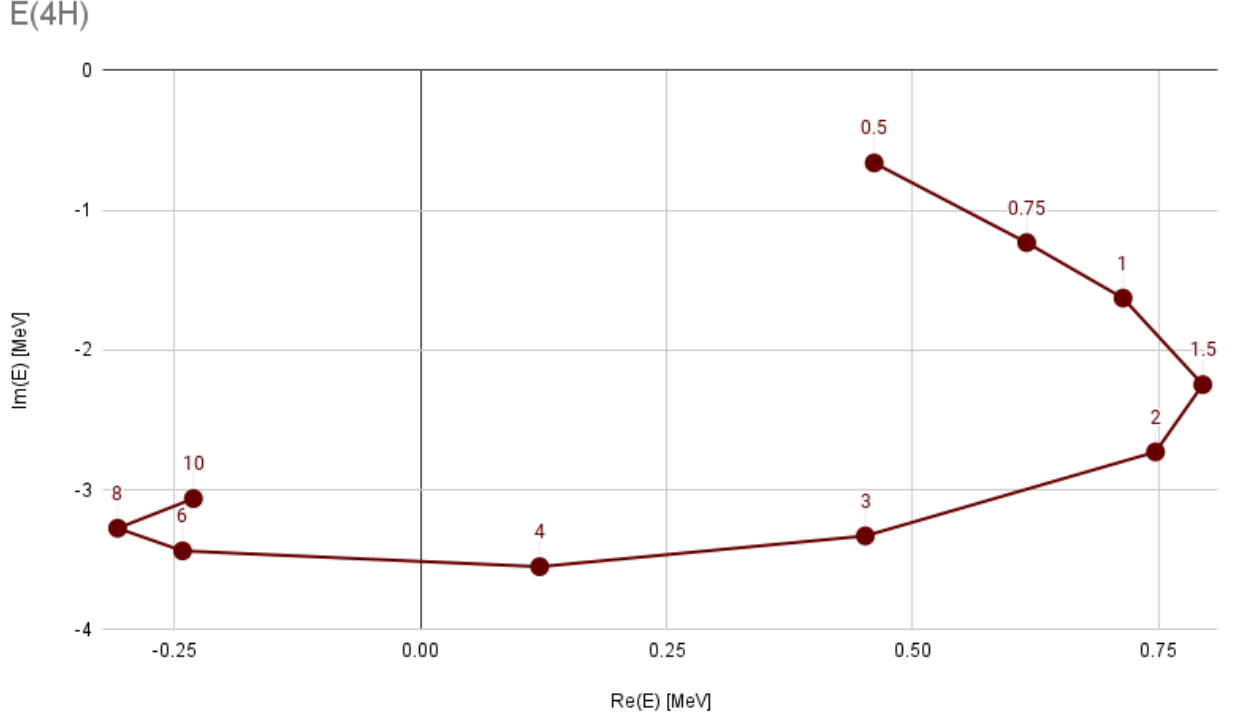
FIG. 2: 1^- resonant pole in ^{4}H

stabilize around $E_{n-t} = -8.7 - i\,3.1$ for cutoffs greater than 6 fm^{-1}. This represents a shallow and broad subthreshold resonance. The presence of such a state and especially its stability (in this case expressed as a pole that does not run to infinite energy increasing the cut-off) is not trivial for the same reasons as one might not expect scattering length/volumes larger than zero. Therefore, this proves that the theory is able to predict shallow states in systems with mixed symmetry. However, the position of the LO EFT pole appears to not be compatible with the physical resonance in ^{4}H: ??? ($E_{n-t} = 8.17 + i\,6.73$). Nonetheless, the theory is only tested at LO where the relevant operators to describe such states are not been yet introduced. It is not in principle problematic that the LO pole is not consistent with the experimental data since including the subleading orders (NLO and N^{2}LO) can, even in a perturbative treatment of the expansion, relocate it in the correct position. However, in this process one should be careful that the insertion of the subleading operators does not shift unreasonably, neither too much nor in the wrong direction, any of the other observables (e.g. the ^4He energy or the $n-^2H$ phaseshifts). At the current knowledge of the authors, no studies have ever been done in this sense and the possibility of a consistent correction of a resonant pole in therms of powerconting hierarchy remains to be demonstrated.

Universality

In the framework of universal systems, in which the two-body scattering length is divergent, the scattering volume of $n-^3H$ follows an identical pattern as before, but with a convergent value of ~ 4 fm^3. This can be compared to the typical coordinate scale of the system, which, in this case, is uniquely identifiable with the three-body scale $R_3 = (-2mE_3/\hbar^2)^{-1/2} \simeq 6$ fm. We find that $(a_1)^{-1/3}/R_3 \simeq 1/4$, which is a small, but still natural ratio.

** here I have some discrepancies (martin A11 is twice Rimas A11) **[martin pole and data for unitarity]**
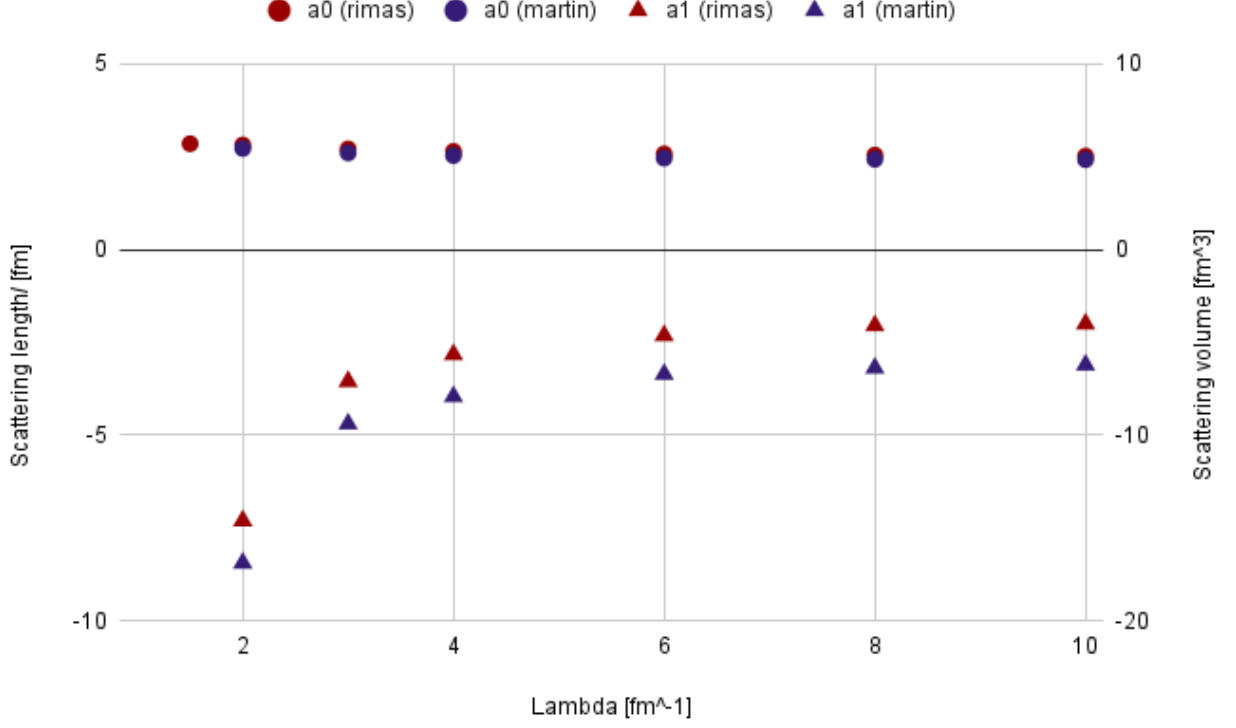
FIG. 3: Temporary: unitary scattering lengths / volume

IV.   CONCLUSION

V.   APPENDIX: RESONATING GROUP METHOD AND INTERACTIONS

The non-relativistic dynamics of the four particles is given by the solutions to

$$\left(-\frac{\hbar^2}{2\mu}\boldsymbol{\Delta}_R - E + \mathcal{V}\right)|\,\Psi\,\rangle \;\Leftrightarrow\; \langle\,\delta\Psi\,\big|\,\hat{H} - E\,\big|\,\Psi\,\rangle = 0 \qquad . \tag{5}$$

The second, viz. the projection/variational equation is equivalent to the Schrödinger equation if $\delta\Psi$ denotes an arbitrary variation of the state. The resonating-group methods expresses the total wave function of this state in the form

$$
\begin{aligned}
\Psi = \mathcal{A}\Big\{ &\sum_i \phi(A_i)\,\phi(B_i)\,\chi_i(\boldsymbol{R}_i) \\
&+ \sum_j \phi(A_j)\,\phi(B_j)\,\phi(C_j)\,\chi_j(\boldsymbol{R}_{j1},\boldsymbol{R}_{j2}) + \sum_k \phi(A_k)\,\phi(B_k)\,\phi(C_k)\,\phi(D_k)\,\chi_j(\boldsymbol{R}_{k1},\boldsymbol{R}_{k2},\boldsymbol{R}_{k3}) \\
&+ \ldots + \sum_m c_m\eta_m \Big\}\,\zeta(\boldsymbol{R}_{\text{c.m.}}) \qquad ,
\end{aligned} \tag{6}
$$

where each term corresponds to a particular fragmentation of the particles into two, three, four, ... cluster. The internal motion of such a cluster of A particles is expanded with a complete set of functions $\phi(A_i)$, and the relative motion between the clusters is encoded in the χ_i's. The last term is included to improve the expansion if the fragment-internal basis is not complete and/or if the cluster expansion is truncated such that a more complicated shape of the state for small separations between the clusters cannot be accounted for.

For the elastic scattering of a neutron off a three-nucleon targets whose ground state is $\Delta\epsilon_{\text{nuclear}} \approx 6.2$ MeV and $\Delta\epsilon_{\text{unitary}} \approx 8.4$ MeV, respectively, below the lowest dissociation thresholds, and the relative energies between the

fragments $E_r \ll \Delta\epsilon$, we chose to express the wave function of the system with a two-cluster, single-channel ansatz without specific distortion:

$$\Psi = \mathcal{A}_{31}\left[\phi(3)\phi(1)\,\chi(\boldsymbol{R})\,\zeta(\boldsymbol{R}_{\text{c.m.}})\right] = \int \mathcal{A}_{31}\left[\phi(3)\phi(1)\,\delta\left(\boldsymbol{R}-\boldsymbol{R}'\right)\zeta(\boldsymbol{R}_{\text{c.m.}})\right]\chi(\boldsymbol{R}')\,d\boldsymbol{R}' \qquad . \tag{7}$$

cf. eq. (9), first term. The parameter representation employed with the second equality in eq. (7) will yield a defining equation for the relative motion independent of the antisymmetrizer $\mathcal{A}$. Assuming an inert triton core allows solely for a variation of the relative wave function:

$$\delta\Psi = \int \delta\chi(\boldsymbol{R}')\,\mathcal{A}_{AB}\left[\phi_A\phi_B\,\delta\left(\boldsymbol{R}-\boldsymbol{R}'\right)\zeta(\boldsymbol{R}_{\text{c.m.}})\right]d\boldsymbol{R}' \equiv \oint \delta a_n \Phi_n \qquad . \tag{8}$$

The latter notation allows for the following concise form of the projection equation

$$\left\langle \oint \delta a_m \Phi_m \,\middle|\, \hat{H}-E \,\middle|\, \oint a_n \Phi_n \right\rangle = 0 \;\to\; \left\langle \phi(3) \,\middle|\, \hat{H}-E \,\middle|\, \mathcal{A}_{31}\left[\chi(\boldsymbol{R}')\,\phi(3)\right]\right\rangle_{\boldsymbol{R}} = 0 \tag{9}$$

where the *ket* subscript average indicates that the average over the relative radius was already taken, and the remaining integrals are over the fragment-internal coordinates. If the cluster-internal states are properly anti-symmetrized, it remains to consider the inter-fragment anti-symmetrization via $\mathcal{A}_{31} = \mathbb{1} - \hat{P}_{14}$. We chose nucleons 1 and 4 to be the neutrons with identical spin orientation, and hence need to consider the permutation of those particles, only. All other permutations $\hat{P}_{ij}$ will yield zero matrix elements because of the orthogonality of the internal states.

Being more explicit, the motion of the two fragments relative to each other is approximated by

$$\int \left\{ \phi(3)\left(-\frac{\hbar^2}{2\mu}\boldsymbol{\Delta}_R - E + B(3) + \mathcal{V}_{31}\right)\mathcal{A}_{31}\left[\phi(3)\,\chi(\boldsymbol{R})\right]\right\}d\boldsymbol{r}_{1,2,3} = 0 \qquad . \tag{10}$$

This expression is further evaluated by: (i) employing the parameter representation, $\chi(\boldsymbol{R}) = \int \delta(\boldsymbol{R}-\boldsymbol{R}')\chi(\boldsymbol{R}')d\boldsymbol{R}'$; (ii) expanding the triton ground state in Gaussians, $\phi(3) = \sum_n^{N_f} c_n \cdot e^{-\alpha_n \Sigma_{i=1}^3 (\boldsymbol{r}_i - \boldsymbol{R}_3)^2}$ with norm $\mathbb{N}_3 = \sum_{i,j=1}^{N_f} c_i c_j \left(\frac{\pi}{\alpha_i + \alpha_j}\right)^{3/2}$; (iii) substituting the leading-order EFT($\not\pi$) potential as inter-cluster interaction,

$$\mathcal{V}_{31} = C(\lambda) \sum_{\substack{i\in A \\ j\in B}} \delta_\lambda^{(3)}\!\left(\boldsymbol{r}_i - \boldsymbol{r}_j\right) + D(\lambda) \sum_{\substack{i,j,k \\ i\in A \Rightarrow j\vee k\in B}} \delta_\lambda^{(3)}\!\left(\boldsymbol{r}_i - \boldsymbol{r}_j\right)\delta_\lambda^{(3)}\!\left(\boldsymbol{r}_i - \boldsymbol{r}_k\right)$$
$$= C(\lambda) \cdot \left(\delta_\lambda^{(3)}\!\left(\boldsymbol{r}_2 - \boldsymbol{r}_4\right) + \delta_\lambda^{(3)}\!\left(\boldsymbol{r}_3 - \boldsymbol{r}_4\right)\right) + D(\lambda) \cdot \left(\delta_\lambda^{(3)}\!\left(\boldsymbol{r}_2 - \boldsymbol{r}_3\right)\delta_\lambda^{(3)}\!\left(\boldsymbol{r}_2 - \boldsymbol{r}_4\right)\right) \qquad ; \tag{11}$$

(iv) performing the action of $\mathcal{A}_{31}$ on ϕ_3 and $\delta(\boldsymbol{R}-\boldsymbol{R}')$; and finally, (v) doing the Gaussian integrals for the triton-internal single-particle coordinates $\boldsymbol{r}_{1,2,3}$. Thereby, one obtains the form

$$(\hat{T}-E)\,\chi(\boldsymbol{R}) + \mathcal{V}^{(1)}(\boldsymbol{R})\,\chi(\boldsymbol{R}) + \int d^{(3)}\boldsymbol{R}'\,\mathcal{V}^{(2)}(\boldsymbol{R},\boldsymbol{R}',E)\,\chi(\boldsymbol{R}') = 0 \qquad . \tag{12}$$

More conveniently, we do express this equation as

$$\mathbb{N}_3 \cdot \left(-\boldsymbol{\Delta}_R - \boldsymbol{p}^2\right)\chi(\boldsymbol{R}) + \sum_{i,j=1}^{N_f} c_i c_j \left[\sum_{n=1}^2 \eta_n^{(ij)}\,e^{-w_n^{(ij)}\boldsymbol{R}^2}\chi(\boldsymbol{R}) - \sum_{n=1}^3 \int \left\{\zeta_n^{(ij)}\hat{\zeta}_n\,e^{-a_n^{(ij)}\boldsymbol{R}^2 - b_n^{(ij)}\boldsymbol{R}\cdot\boldsymbol{R}' - c_n^{(ij)}\boldsymbol{R}'^2}\right\}\chi(\boldsymbol{R}')d\boldsymbol{R}'\right] = 0 \tag{13}$$

with $\hat{\eta}_n, \hat{\zeta}_n, w_n, a_n, b_n, c_n$ dependent upon, (i) the low-energy constants: $C(\lambda), D(\lambda)$, (ii) the triton-expansion parameters: α_n, c_n, (iii) the regulator parameter: λ, and (iv) the relative momentum: $\boldsymbol{p}^2 = 2\mu E$, as given in table (II).

The character of the interaction is expected to depend strongly on the spatial symmetry of the wave function, and as the parities of the triton core and the point neutron are positive, the overall parity is set by the relative motion χ. In

n	$\eta^{(ij)}$	$w^{(ij)}$		
1	$\dfrac{2C(\lambda)}{\left[2(\alpha_i+\alpha_j)(3\alpha_i+3\alpha_j+2\lambda)\right]^{3/2}}$	$\dfrac{3(\alpha_i+\alpha_j)\lambda}{3(\alpha_i+\alpha_j)+2\lambda}$		
2	$\dfrac{D(\lambda)}{\left[6(\alpha_i+\alpha_j)^2+16\lambda(\alpha_i+\alpha_j)+2\lambda^2\right]^{3/2}}$	$\dfrac{3(\alpha_i+\alpha_j)\lambda((\alpha_i+\alpha_j)+2\lambda)}{3(\alpha_i+\alpha_j)^2+8(\alpha_i+\alpha_j)\lambda+\lambda^2}$		

n	$\zeta^{(ij)}\otimes\hat\zeta$	$a^{(ij)}$	$b^{(ij)}$	$c^{(ij)}$
1	$\dfrac{\hbar^2}{2\mu}\dfrac{3^3}{2^6}\dfrac{1}{[2(\alpha_i+\alpha_j)]^{3/2}}\otimes\left(-\boldsymbol{\Delta}_R-\boldsymbol{p}^2\right)$	$\dfrac{3}{32}(\alpha_i+9\alpha_j)$	$\dfrac{9}{16}(\alpha_i+\alpha_j)$	$\dfrac{3}{32}(9\alpha_i+\alpha_j)$
2	$-\dfrac{3^3}{2^5}\dfrac{C(\lambda)}{[2(\alpha_i+\alpha_j)+\lambda]^{3/2}}\otimes\mathbb{1}$	$\dfrac{3(\alpha_i^2+9\alpha_j^2+10\alpha_i\alpha_j+\lambda(14\alpha_i+18\alpha_j))}{16(2(\alpha_i+\alpha_j)+\lambda)}$	$\dfrac{18(\alpha_i+\alpha_j)(\alpha_i+\alpha_j)+2\lambda}{16(2(\alpha_i+\alpha_j)+\lambda)}$	$\dfrac{3(9\alpha_i^2+\alpha_j^2+10\alpha_i\alpha_j+\lambda(6\alpha_i+2\alpha_j))}{16(2(\alpha_i+\alpha_j)+\lambda)}$
3	$-\dfrac{3^3}{2^6}\dfrac{D(\lambda)}{[2(\alpha_i+\alpha_j)+5\lambda]^{3/2}}\otimes\mathbb{1}$	$\dfrac{3(\alpha_i^2+9\alpha_j^2+10\alpha_i\alpha_j+\lambda(16\alpha_i+36\alpha_j)+27\lambda^2)}{16(2(\alpha_i+\alpha_j)+5\lambda)}$	$\dfrac{18((\alpha_i+\alpha_j)^2+4\lambda(\alpha_i+\alpha_j)+3\lambda^2)}{16(2(\alpha_i+\alpha_j)+5\lambda)}$	$\dfrac{3(9\alpha_i^2+\alpha_j^2+10\alpha_i\alpha_j+\lambda(24\alpha_i+4\alpha_j)+3\lambda^2)}{16(2(\alpha_i+\alpha_j)+5\lambda)}$

TABLE II: Local (η,w) and non-local (ζ,a,b,c) components of the resonating-group eq. (13).

order to investigate the parity dependence, we project into partial waves: Expanding $\chi(\boldsymbol{R})=R^{-1}\sum_{lm}\phi_{lm}(R)Y_{lm}(\hat{\boldsymbol{R}})$ and projecting from the left with $R\int d^2\hat{\boldsymbol{R}}\,Y_{lm}^*(\hat{\boldsymbol{R}})$ before substituting

$$e^{-b\boldsymbol{R}\cdot\boldsymbol{R}'}=4\pi\sum_{LM}i^L j_L(ibRR')Y_{LM}^*(\hat{\boldsymbol{R}})Y_{LM}(\hat{\boldsymbol{R}}')\ ;\ \ \boldsymbol{R}\cdot\boldsymbol{R}'=-\sqrt{3}\left[\boldsymbol{R}_p\otimes\boldsymbol{R}'_{-p}\right]^{00}=\frac{4\pi}{3}RR'\sum_p(-)^p Y_{1p}Y'_{1-p}$$

and $\boldsymbol{r}_m=\sqrt{\frac{4\pi}{3}}rY_{1,m}(\hat{\boldsymbol{r}})$ yields

$$0=\mathbb{N}_3\cdot\left(\partial_R^2-\frac{l(l+1)}{R^2}+\boldsymbol{p}^2\right)\phi_{lm}(R)-\frac{2\mu}{\hbar^2}\sum_{i,j=1}^{N_f}c_ic_j\left(\sum_{n=1}^2\eta_n^{(ij)}\,e^{-w_n^{(ij)}R^2}\phi_{lm}(R)\right.$$

$$-\int dR'\,\phi_{lm}(R')\,(4\pi RR')\left[\zeta_1^{(ij)}\cdot e^{-a_1^{(ij)}R^2-c_1^{(ij)}R'^2}\cdot\left\{\left[-(4(a_1^{(ij)})^2R^2+(b_1^{(ij)})^2R'^2-2a_1^{(ij)})+\frac{l(l+1)}{R^2}-\frac{2\mu}{\hbar^2}E\right]i^l j_l(ib_1^{(ij)}RR')\right.\right.$$

$$\left.\left.-(4a_1^{(ij)}b_1^{(ij)})\cdot RR'\cdot\sum_L i^L j_L(ib_1^{(ij)}RR')\,\hat{L}\,\hat{l}\begin{pmatrix}L&1&l\\0&0&0\end{pmatrix}^2\triangle_{L1l}\right\}+\sum_{n=2}^3\zeta_n^{(ij)}i^l j_l(ib_nRR')\cdot e^{-a_n^{(ij)}R^2-c_n^{(ij)}R'^2}\right]\right) \quad (14)$$

with a 3-j symbol $\neq 0\Leftrightarrow L+1+l=$ even, and $\triangle_{j_1j_2j_3}\neq 0\Leftrightarrow j_3=|j_1-j_2|,\ldots,j_1+j_2$. From this equation, we obtain solutions for S- and P-waves on a discrete, equidistant coordinate grid: $R,R'\in\{r_0,r_0+\epsilon,r_0+2\epsilon,\ldots,\underbrace{r_0+N_{\mathrm{grid}}\epsilon}_{=:r_{N_{\mathrm{grid}}+1}}\}$. We chose a maximal grid dimension such that for $R(')=r_{N_{\mathrm{grid}}+1}$ both local and non-local interactions vanish. Thence, we solve eq. (14) for the *principal-value* wave function $(\phi^{(P)})$ with the boundary condition

$$\phi_{l,p}^{(P)}(R)\overset{R\to\infty}{\simeq}\sin\left(pR-\frac{\pi l}{2}\right)+K_l\cdot\cos\left(pR-\frac{\pi l}{2}\right) \tag{15}$$

$$=\lim_{pR\to\infty}\left[u_l(pR)\right]+\tan\delta_l\cdot\lim_{pR\to\infty}\left[v_l(pR)\right]=\begin{cases}l=0:\ \sin(pR)-\tan\delta_l\cos(pR)\\l=1:\ \frac{\sin(pR)}{pR}-\cos(pR)-\tan\delta_l\left[\frac{\cos(pR)}{pR}+\sin(pR)\right]\end{cases} \tag{16}$$

For the Riccati-Bessel, $u_l(z)=zj_l(z)$, and the Riccati-Neumann Functions, $v_l(z)=zn_l(z)$, we use [] as reference, where $j_l(n_l)$ is the proper spherical Bessel(Neumann) function. Note, the relation between the Neumann and the spherical Bessel function of the second kind: $n_l(z)=(-)^l y_l(z)$. Now, we obtain the phase shifts from

$$\tan\delta_l=\frac{\phi_{l,p}^{(P)}(r_{N_{\mathrm{grid}}+1})}{v_l(pr_{N_{\mathrm{grid}}+1})}-\frac{u_l(pr_{N_{\mathrm{grid}}+1})}{v_l(pr_{N_{\mathrm{grid}}+1})}\quad . \tag{17}$$
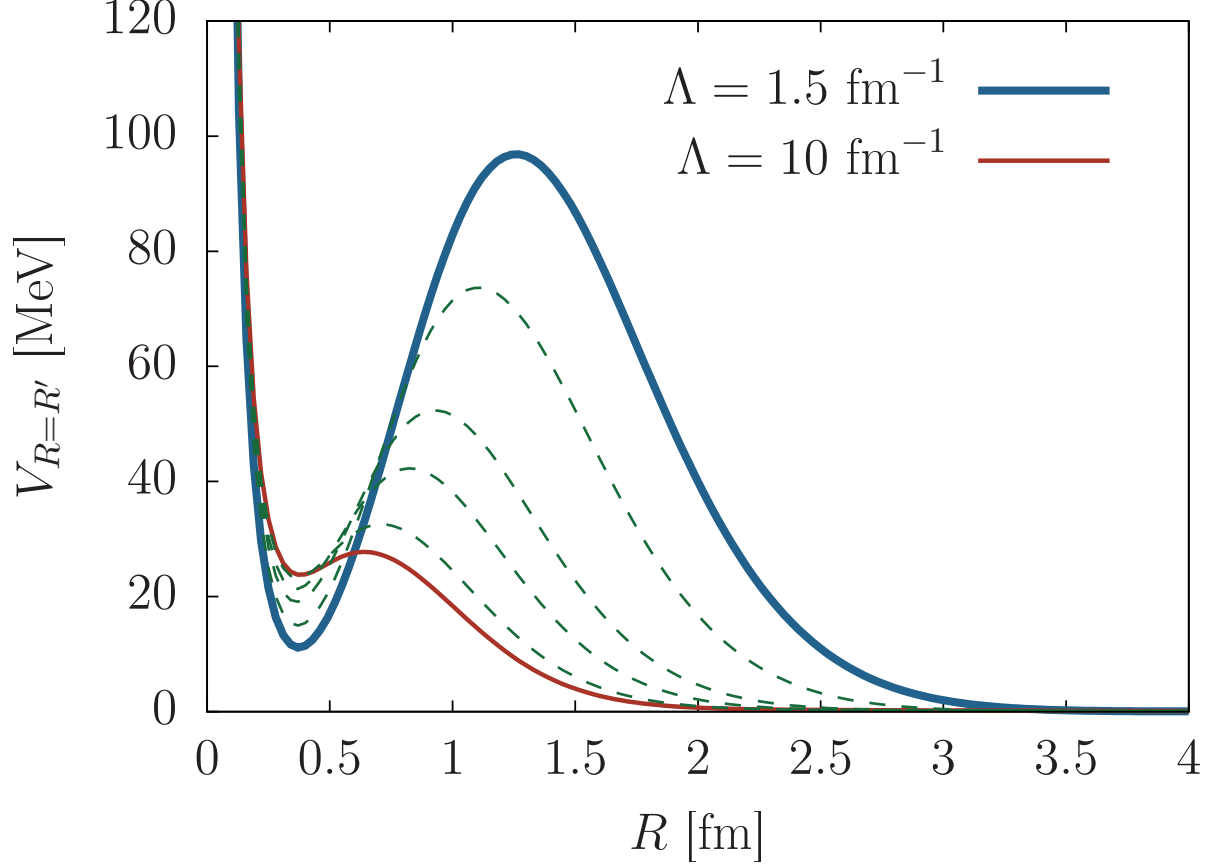
FIG. 4: Two-fragment potential as a function of the distance between a neutron and the center of mass of a triton. The plot shows the P-wave component of the interaction including local and non-local part of the kinetic-, pair-, and three-body interactions. The non-local parts are evaluated at $R = R'$. The height of the potential's barrier shrinks continuously from the smallest cutoff (fat blue) to the largest (red), with intermediate values represented by green, dashed curves.
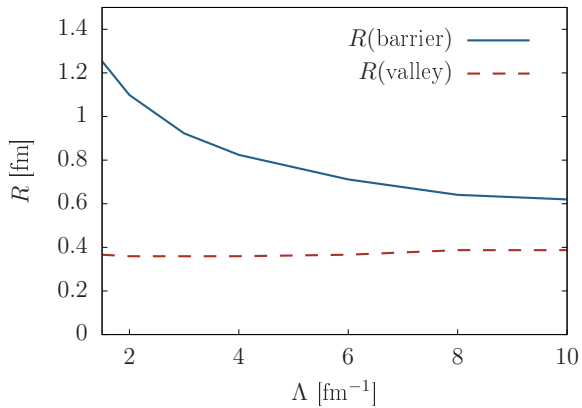

FIG. 5: Locus of the valley (red, dashed) and the barrier (blue, solid) of the effective resonating-group interaction (fig. (4)) as a function of the regulator parameter λ.
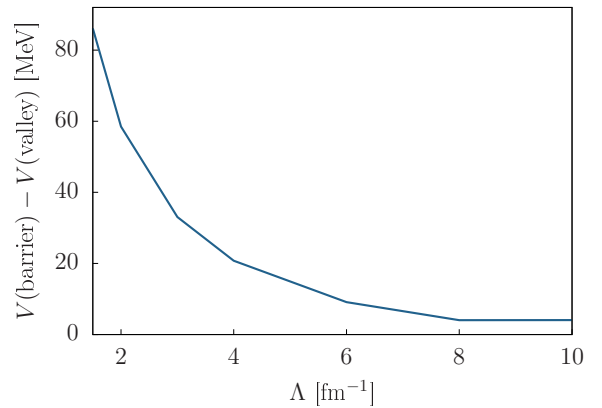

FIG. 6: Regulator dependence of the difference between the first local maximum of the effective resonating-group potential (fig. (4)) and its first local minimum.